Food & Function

ROYAL SOCIETY OF CHEMISTRY

PAPER

View Article Online
View Journal | View Issue

Cite this: *Food Funct.*, 2026, **17**, 3372

Comparative evaluation of the short-chain fatty acids formate, propionate, and valerate on intestinal barrier maturation and bone development in neonatal mice

Xue Yang,†[a,b,c] Xinke Li,†[a,b,c] Xuan Zhang,[a,b,c] Lu Meng,[a,b,c] Jiaqi Wang[a,b,c] and Nan Zheng *[a,b,c]

Short-chain fatty acids (SCFAs) are key microbial metabolites that support intestinal and skeletal development, yet their coordinated effects during early life remain poorly defined. In this study, neonatal mice were administered SCFAs for 28 days to evaluate their impacts on growth, intestinal barrier integrity, immune modulation, bone development, and gut microbiota composition. Valerate supplementation significantly increased body weight and intestinal length. It enhanced the villus structure, crypt depth, and goblet cell number, alongside upregulation of tight junction and mucin genes, indicating improved barrier function. Valerate and propionate also promoted the expression of interleukin-4 (IL-4) and interleukin-10 (IL-10) and reduced pro-inflammatory cytokines, suggesting an immunomodulatory shift. In the skeletal system, valerate improved the microarchitecture, increased bone mineral density (BMD), and upregulated osteogenic genes runt-related transcription factor 2 (Runx2), fibroblast growth factor receptor 1 (FGFR1), and growth hormone receptor (GHR). Microbiota profiling showed enrichment of several genera (*e.g.*, *Fructobacillus*, *Pantoea*, and *Ralstonia*) that correlated with intestinal and bone parameters. Collectively, these data indicate that valerate supplementation is associated with concurrent improvements in neonatal intestinal and skeletal outcomes, accompanied by shifts in microbiota and changes related to the barrier and immune systems; however, causal links among these intermediate steps remain to be established.

Received 11th December 2025,
Accepted 26th January 2026

DOI: 10.1039/d5fo05394c

rsc.li/food-function

Introduction

The gut microbiota is essential for maintaining host health, influencing not only intestinal functions but also immune modulation and skeletal metabolism.[1–3] Among its key metabolites, short-chain fatty acids (SCFAs), primarily generated through microbial fermentation of dietary fibers, have emerged as central mediators of gut–organ communication.[4,5] SCFAs play a fundamental role in preserving gut health by strengthening epithelial barrier integrity, regulating immune signaling, and sustaining microbial homeostasis.[4,6] Moreover, accumulating evidence shows that SCFAs support bone development by modulating bone metabolism and mineral balance.[7,8]

The neonatal period represents a critical window for gut and skeletal development.[9,10] Maturation of the intestinal barrier and rapid bone mineralization are essential for ensuring healthy growth. While the gut facilitates nutrient uptake and contributes to immune defense, the skeleton provides structural support and regulates calcium–phosphorus balance.[11,12] Proper development of both systems during early life has lasting impacts on health, underscoring the importance of investigating their interplay to inform early-life nutritional strategies and disease prevention.

An expanding body of evidence highlights the critical contribution of SCFAs to early-life intestinal maturation and immune homeostasis. They enhance barrier function by upregulating tight junction proteins (claudin-1, occludin, and ZO-1) and stimulating mucin (*e.g.*, MUC2) secretion from goblet cells.[13] Additionally, SCFAs exert immunomodulatory effects by suppressing inflammatory pathways like NF-κB and inducing anti-inflammatory cytokines such as IL-10, primarily through G protein-coupled receptor (GPCR) activation and histone deacetylase (HDAC) inhibition.[14,15] Consistently, inhibition of the TRAF6-NF-κB axis has been linked to improved intestinal inflammatory outcomes in colitis models.[16] During

[a]*Laboratory of Quality Safety Control for Milk and Dairy Products of Ministry of Agriculture and Rural Affairs, Institute of Animal Sciences, Chinese Academy of Agricultural Sciences, Beijing 100193, China. E-mail: zhengnan@caas.cn*
[b]*Laboratory of Quality and Safety Risk Assessment for Dairy Products of Ministry of Agriculture and Rural Affairs (Beijing), Institute of Animal Sciences, Chinese Academy of Agricultural Sciences, Beijing 100193, China*
[c]*Key Laboratory of Dairy Quality Digital Intelligence Monitoring Technology, State Administration for Market Regulation, Shanghai 201114, China*
†These authors contributed equally to this work.

early life, SCFAs also act as signaling molecules mediating host–microbe–milk crosstalk, facilitating epithelial maturation and microbiota stabilization.[17] However, the specific functions of SCFAs in neonatal intestinal development remain incompletely understood.

Recent studies also suggest that SCFAs regulate bone development by enhancing osteogenic processes and suppressing osteoclast differentiation, thereby improving the bone density and structure.[7,8] Butyrate and propionate have been shown to enhance bone formation *via* HDAC inhibition and Wnt signaling activation,[8] and support calcium homeostasis by promoting intestinal calcium absorption and solubility.[18] SCFAs also stimulate IGF-1 signaling and GPR41-mediated pathways that influence bone remodeling.[19,20] They also suppress osteoclastogenesis by downregulating TRAF6 and NFATc1 expression in precursor cells.[7] However, most current evidence derives from adult or disease models, and little is known about how different SCFAs influence bone development during the neonatal period.

Although acetate, propionate, and butyrate are typically regarded as the major SCFAs in adult gut ecosystems, their early-life microbial metabolite profiles differ substantially. Longitudinal infant studies have shown that formate can be elevated during early infancy and is linked to *Bifidobacteriales*-dominant communities, whereas propionate and butyrate tend to increase later during microbiota maturation.[21] In addition, propionate is a well-characterized SCFA with systemic bioavailability and has been implicated in immune regulation and bone-related pathways (*e.g.*, IGF-1-associated mechanisms).[22] By contrast, valerate (C5) is less studied in early life but is increasingly recognized as a bioactive microbial metabolite; it can be generated *via* microbial cross-feeding and has been reported to support intestinal barrier function, and C3–C5 SCFAs (including propionate and valerate) show relatively high potency at SCFA receptors such as FFAR3/GPR41.[23] Collectively, these considerations motivated us to focus on formate (an early-life-relevant microbial organic acid), propionate (a canonical SCFA with established host signaling relevance), and valerate (an underexplored C5 SCFA with emerging gut-related bioactivity) to compare their effects on neonatal gut and bone development.

To fill this research gap, we investigated the effects of three SCFAs formate, propionate, and valerate, on gut and bone development in neonatal mice. We systematically assessed their impacts on body growth, intestinal barrier integrity, immune responses, bone morphology, and gut microbiota composition. Furthermore, we explored correlations between SCFA-induced microbial shifts and host phenotypes to uncover regulatory patterns within the early-life gut–bone axis.

Materials and methods

Animals and housing

All experimental procedures involving animals were reviewed and approved by the Animal Ethics Committee of the Chinese Academy of Agricultural Sciences (approval number: IAS2022-108), following ethical guidelines for animal treatment. Newborn C57BL/6J mice were obtained from Cyagen (Gu'an) Biotechnology Co., Ltd. All mice were housed in an SPF (Specific Pathogen-Free) barrier system at the Suzhou Taicang Animal Experiment Platform under controlled conditions (12-hour light/dark cycle, 22 ± 2 °C, and 50 ± 10% humidity), with standard laboratory chow and water provided *ad libitum*. Pups of both sexes were used; sex was not treated as an experimental factor because pups were randomly allocated prior to sex determination. Because the litter size varied naturally and was not predetermined, pups were assigned to the seven experimental groups using a litter-stratified randomization approach: within each litter, pups were randomly allocated across groups as evenly as possible, and allocation across litters continued until the target sample size was reached. Ultimately, 42 pups were included for analysis (n = 6 per group), and each group contained offspring derived from multiple dams to minimize potential maternal/litter effects. Weaning occurred at postnatal day (PND) 18; thereafter, dams were removed and pups remained in the same cage (no re-caging).

Study design and SCFA administration

The intervention began at PND1, with pups randomly assigned to experimental groups.

The experimental groups were as follows:

Formic acid: 900 mg per kg body weight (BW) (SF-900) and 1400 mg per kg BW (SF-1400).

Propionic acid: 2 mg per kg BW (SP-2) and 200 mg per kg BW (SP-200).

Valeric acid: 5 mg per kg BW (SV-5) and 20 mg per kg BW (SV-20).

The control group (CTL) received physiological saline.

The SCFAs were sodium formate (Aladdin, S104884-5g, 99.998%), sodium propionate (Sigma-Aldrich, P1880-100G, ≥99.0%), and sodium valerate (Aladdin, S194180-5 g, ≥97%). Doses were determined based on SCFA concentrations measured in human milk, bovine milk, and infant formula (Table S1A) and converted to mouse-equivalent exposures using standard body surface area (BSA) scaling. Briefly, infant-equivalent intake (mg kg^{-1} day^{-1}) was estimated from measured milk concentrations assuming a daily intake of 750 mL and an infant body weight of 6.5 kg and then converted to a mouse-equivalent dose using a mouse-to-human BSA conversion factor of 9.1. Final experimental doses were selected to approximate the calculated mouse-equivalent exposure range and were rounded to practical dosing levels (Table S1B).

Animal treatment and sample collection

Gavage was administered daily for PND1–PND28, covering both the neonatal period and part of the *peri*-weaning period, during which their body weight was monitored at 3-day intervals. Weaning occurred at PND18, and the pups remained in the same cage. The day before dissection, fresh stool samples were collected using a metabolic cage. Following carbon dioxide anesthesia, blood samples were collected by cardiac puncture

and serum was obtained by centrifugation (10 000 rpm, 6 min). After euthanasia by cervical dislocation, the major organs, intestines, femora, and tibiae were promptly harvested for subsequent biochemical and histological analyses.

Measurement of body length and tail length

Body length and tail length were measured using a digital caliper. Body length was defined as the distance from the tip of the nose to the base of the tail, and tail length was measured from the base of the tail to the tail tip. All measurements were taken to the nearest 0.01 mm.

Determination of the organ index

The brain, heart, liver, kidneys, spleen, and thymus were harvested and rinsed three times with phosphate-buffered saline (PBS) to remove surface blood and impurities. Any surrounding adipose tissue was carefully dissected away. Each organ was then weighed, and the organ index was calculated using the following formula:

$$\text{Organ index } (\%) = (\text{organ weight}/\text{body weight}) \times 100.$$

Histological observation

Intestinal samples were fixed in 4% paraformaldehyde, embedded in paraffin, and sliced into sections for microscopic examination. Tissue morphology was visualized using hematoxylin and eosin (H&E) staining. To assess the distribution of acidic mucus in the jejunum, Alcian Blue–Periodic Acid Schiff (AB-PAS) staining was used, with acidic mucus appearing blue. Stained sections were scanned using a digital pathology scanner, and representative images were randomly selected. Morphometric analysis was conducted using ImageJ software: villus height and crypt depth were measured manually, and goblet cells were counted in the stained regions. All measurements were averaged to ensure accuracy.

Micro-CT analysis and bone mineral density determination of femurs

The left femurs were scanned using micro-computed tomography (micro-CT) to evaluate the bone mineral density (BMD) and microstructure. Scanning was performed using a high-resolution micro-CT system (SkyScan 1275, Bruker) with a voxel size of 9 μm, 400 layers, 46 kV voltage, and 75 μA current. Three-dimensional reconstruction was conducted using NRECON software. Quantitative analysis was carried out using CTAN software.

FITC–dextran permeability assay

Each mouse was fasted overnight prior to gavage and then orally administered 0.2 mL of 40 kDa fluorescein isothiocyanate–dextran (FITC–dextran, Sigma-Aldrich, Spain) at a dose of 200 mg per kg BW. The mice were maintained for 3 h before euthanasia. Blood samples were collected, and serum fluorescence intensity was measured using an Infinite M200 multimode microplate reader. The entire gastrointestinal tract was excised and imaged *ex vivo* using an Invivosmart LF imaging system (VLEWORKS, USA).

Determination of serum inflammatory cytokines and metabolic markers

Serum levels of lipopolysaccharide (LPS), D-lactic acid, C-terminal peptide of type I collagen (CTX-1), N-terminal peptide of type I collagen (PINP), interleukin-4 (IL-4), interleukin-10 (IL-10), interleukin-6 (IL-6), interleukin-1β (IL-1β), and tumor necrosis factor-α (TNF-α) were quantified using commercially available ELISA kits (Beijing Xinso Biotechnology Co., Ltd).

Real-time quantitative (RT)-PCR analysis

Total RNA was isolated from tissue with a Tissue RNA Extraction Kit 2.0 Plus using a VNP-96P automated nucleic acid extraction system (Vazyme, China) in accordance with the manufacturer's protocol. High-purity RNA was obtained through lysis, isolation, and washing. cDNA synthesis was performed in a 10 μL reaction volume using a commercial reverse transcription kit. RT-qPCR was conducted using a QuantStudio 3 PCR system (Thermo Fisher Scientific) with gene-specific primers (Table S2). PCR conditions were optimized based on the kit's instructions. The $2^{-\Delta\Delta Ct}$ algorithm was applied to determine relative transcript levels with the corresponding CTL group as the calibrator. All reactions were performed in triplicate for technical replication, with six biological replicates per group to ensure data reliability.

16S rDNA amplicon sequencing of fecal microbiota

Fecal DNA was extracted and sequenced by Guangzhou Base Biotechnology Co., Ltd. The V3–V4 region of the bacterial 16S rRNA gene was amplified using 341F (5′-CCTACGGGNGGCWGCAG-3′) and 806R (5′-GGACTACHVGGGTWTCTAAT-3′) primers, and PCR products were verified by agarose gel electrophoresis. Amplicons were pooled and sequenced on the Illumina MiSeq platform (Illumina, San Diego, CA, USA). Raw paired-end reads were quality-filtered using fastp (v0.18.0) (removing reads with adapter contamination, ≥10% ambiguous bases, or >50% bases with $Q \leq 20$) and merged using FLASH (v42) (minimum overlap 10 bp and maximum mismatch rate 2%). Clean tags were obtained by additional stringent filtering (truncation at three consecutive low-quality bases, $Q \leq 3$, and removal of reads retaining <75% of the original length). OTUs were clustered at 97% similarity using UPARSE in USEARCH (v11.0.667), with the most abundant sequence as the representative sequence, and chimeras were removed using UCHIME. Taxonomy was assigned using the RDP classifier (v2.2) against SILVA (v138.1) (confidence threshold 80%). The OTU table was rarefied to the minimum sequencing depth across samples (50 000 reads per sample) prior to downstream analyses. Diversity and community composition analyses were conducted in QIIME2 (*via* Omicsmart, https://www.omicsmart.com).

Statistical analysis

The results are expressed as mean ± SD. For longitudinal bodyweight measurements, differences over time were analyzed by two-way repeated-measures ANOVA (treatment × time) with Geisser–Greenhouse correction, followed by Dunnett's multiple

comparison tests *versus* the control group at each time point. For non-microbiota variables involving comparisons among more than two groups, one-way ANOVA followed by Tukey's multiple comparisons *post-hoc* test was used for normally distributed data. For gut microbiota data, the Wilcoxon test was used to compare groups. Statistical significance was defined as $*p < 0.05$, $**p < 0.01$, $***p < 0.001$, and $****p < 0.0001$.

Results

SCFAs promote neonatal body growth and intestinal elongation

As illustrated in Fig. 1A, neonatal mice were supplemented with SCFAs, resulting in enhanced postnatal growth. Longitudinal body-weight analysis (two-way repeated-measures ANOVA, treatment × time) indicated a significant treatment effect over time, with group differences emerging from day 12 onward (Fig. 1B, Table S3). At the endpoint (day 30), body weight was higher in the SP-2, SP-300, SV-5, and SV-20 groups compared with CTL (Fig. 1B). Body length was also significantly increased in the SP-2, SV-5, and SV-20 groups (Fig. 1C), whereas tail length remained unchanged (Fig. 1D). A notable elongation of the intestine was observed following valeric acid treatment (SV-5 and SV-20) (Fig. 1E). Organ index analysis revealed a decreasing trend in the spleen index in the SF-1400 group and an increase in the SV-20 group, while indices of other organs remained unchanged (Fig. S1A–F).

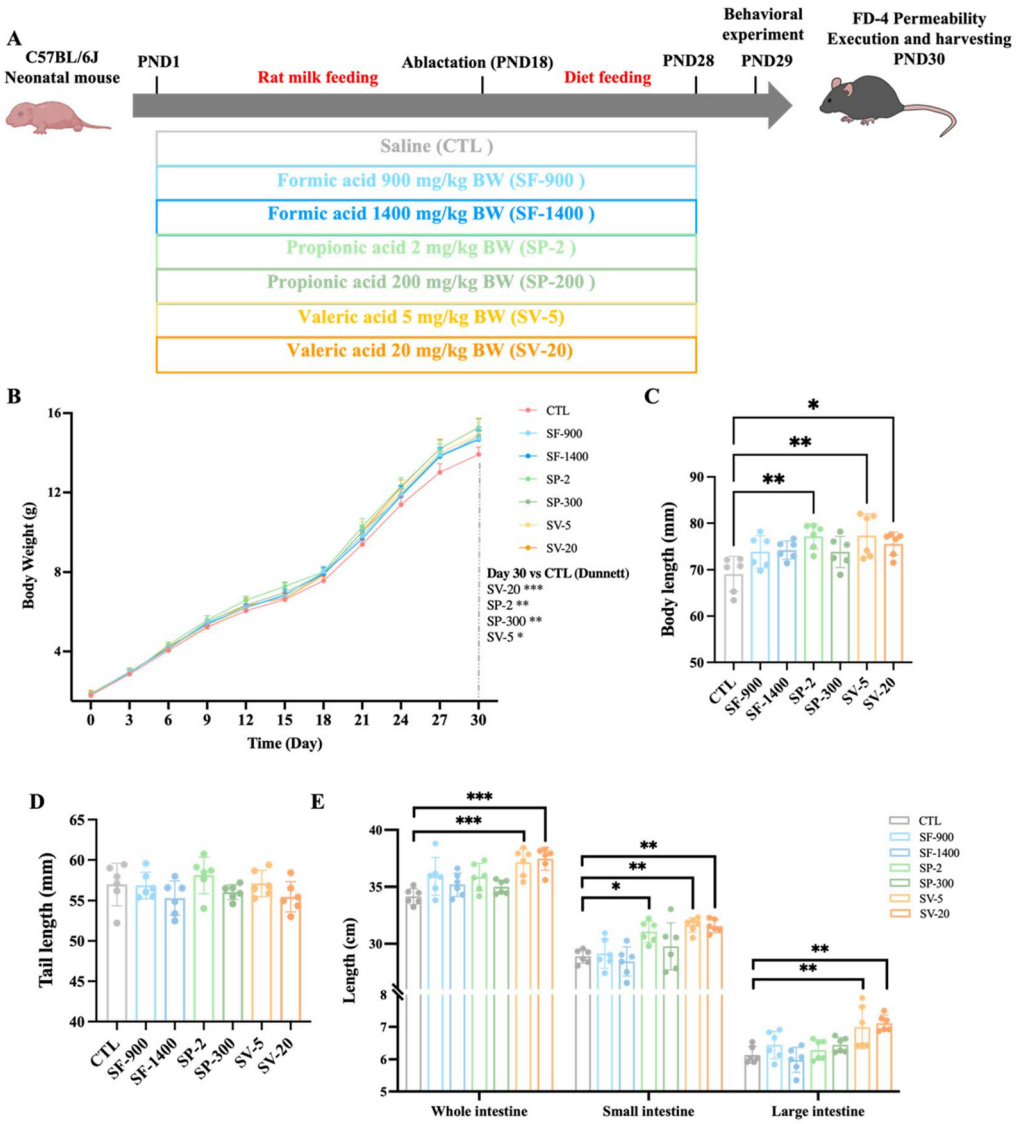

Fig. 1 Effects of SCFAs on neonatal mice body growth and intestinal elongation. (A) Experimental design and groups. (B) Changes in body weight from day 0 to day 30 (two-way repeated-measures ANOVA with Geisser–Greenhouse correction; Dunnett's multiple comparisons *vs*. CTL; significance annotated at day 30). (C) Body length. (D) Tail length. (E) Intestinal length of the mice, with significance levels labeled: $*p < 0.05$, $**p < 0.01$, and $***p < 0.001$ ($n = 6$).

SCFAs enhance intestinal function and barrier integrity

Effect on intestinal motility and permeability. Intestinal permeability and motility were evaluated using the FITC–dextran assay. The SCFA-treated mice showed significantly improved intestinal motility, as evidenced by an increased propulsion rate of the fluorescent tracer (Fig. 2A). The serum fluorescence levels were notably reduced in the SV-5 and SV-20 groups (Fig. 2B), indicating enhanced intestinal barrier function. Additionally, the serum levels of LPS and D-lactic acid were reduced in the SV-20 mice (Fig. 2C and D), reinforcing the role of valeric acid in enhancing intestinal barrier integrity.

Effects on barrier-related gene expression and histology. To further assess barrier integrity, the expression levels of key barrier-related genes claudin-1, occludin, MUC1, MUC2, and ZO-1 were measured in both the jejunum and colon. In the jejunum, claudin-1 and occludin expression was significantly upregulated in the SP-200 and SV-20 groups (Fig. 3A and B). Mucin 1 and Mucin 2 levels were elevated following valeric acid treatment (SV-5 and SV-20) (Fig. 3C and D). ZO-1 expression was significantly increased in the SP-200, SV-5, and SV-20 groups (Fig. 3E). Similarly, in the colon, these barrier-related genes were markedly upregulated in response to valeric acid treatment (Fig. 3F and G), suggesting that valeric acid may enhance intestinal barrier integrity through modulation of the tight junction and mucin-related gene expression.

Histological analysis showed a well-preserved epithelial morphology across all SCFA-treated groups. HE staining revealed intact epithelial structures (Fig. 4A), while AB-PAS staining showed expanded mucus coverage and more goblet cells in the colon of the SV-20 group. Quantitative analysis confirmed significantly elongated villi, deeper crypts, and a higher villus-to-crypt ratio in the SV-20 group in the jejunum (Fig. 4B and C). Additionally, a notable increase in goblet cells was observed in both villi and crypts of the colon (Fig. 4D and E), suggesting enhanced secretory capacity and epithelial renewal.

SCFAs modulate immune responses in neonatal mice

To assess the immunomodulatory effects of SCFAs, serum cytokines were measured. Propionic acid and valeric acid treatments significantly elevated the levels of the anti-inflammatory cytokines IL-4 and IL-10 (Fig. 5A and B). In contrast, valeric acid markedly reduced the concentrations of the pro-inflammatory mediators IL-6 and TNF-α (Fig. 5C and D). The IL-1β levels showed a non-significant downward trend across all groups (Fig. 5E).

SCFAs influence gut microbiota composition

To determine whether SCFA supplementation reshapes the neonatal gut microbiota, we performed 16S rRNA sequencing across the control and the formate-, propionate-, and valerate-treated mice (Fig. 6; Fig. S3 and S4). Microbiota profiles for the valerate groups are shown in Fig. 6, while equivalent analyses for the formate and propionate groups are provided in Fig. S3 and S4. Analysis of α-diversity indices revealed no significant differences between the treatment and control groups (Fig. 6A–E). However, PLS-DA analysis demonstrated clear separation of microbial clusters, indicating distinct microbial profiles between the groups (Fig. 6F). Firmicutes and Bacteroidetes predominated the microbial community at the phylum level (Fig. 6G). At the genus

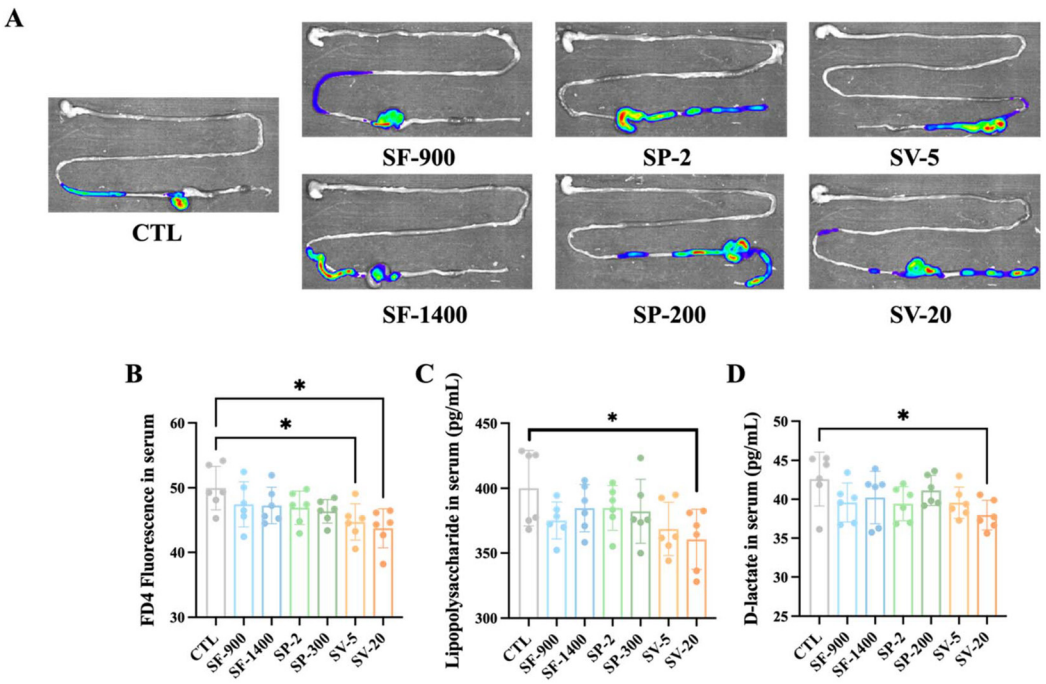

Fig. 2 Effects of SCFAs on intestinal development in neonatal mice. (A) Representative images of intestinal *in vitro* imaging. (B) The content of FD4 in serum. (C and D) The levels of LPS and D-lactic acid in serum. Data were expressed as mean ± standard deviation (mean ± SD), and differences between groups were assessed by one-way ANOVA followed by Tukey's multiple comparisons test: *$p < 0.05$, **$p < 0.01$, ***$p < 0.001$, and ****$p < 0.0001$ ($n = 6$).

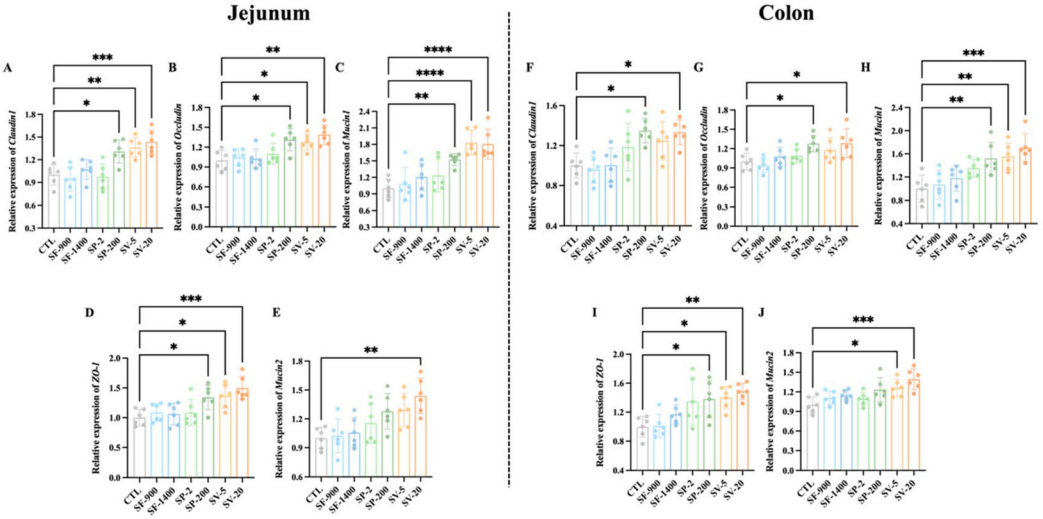

Fig. 3 Effects of SCFAs on the intestinal barrier-related gene expression in neonatal mice. (A–E) Relative expression of claudin, occludin, Mucin 1, Mucin 2, and ZO-1 in the jejunum. (F–J) Relative expression of claudin, occludin, Mucin 1, Mucin 2, and ZO-1 in the colon. Data were expressed as mean ± standard deviation (mean ± SD), and differences between groups were assessed by one-way ANOVA followed by Tukey's multiple comparisons test: *$p < 0.05$, **$p < 0.01$, ***$p < 0.001$, and ****$p < 0.0001$ ($n = 6$).

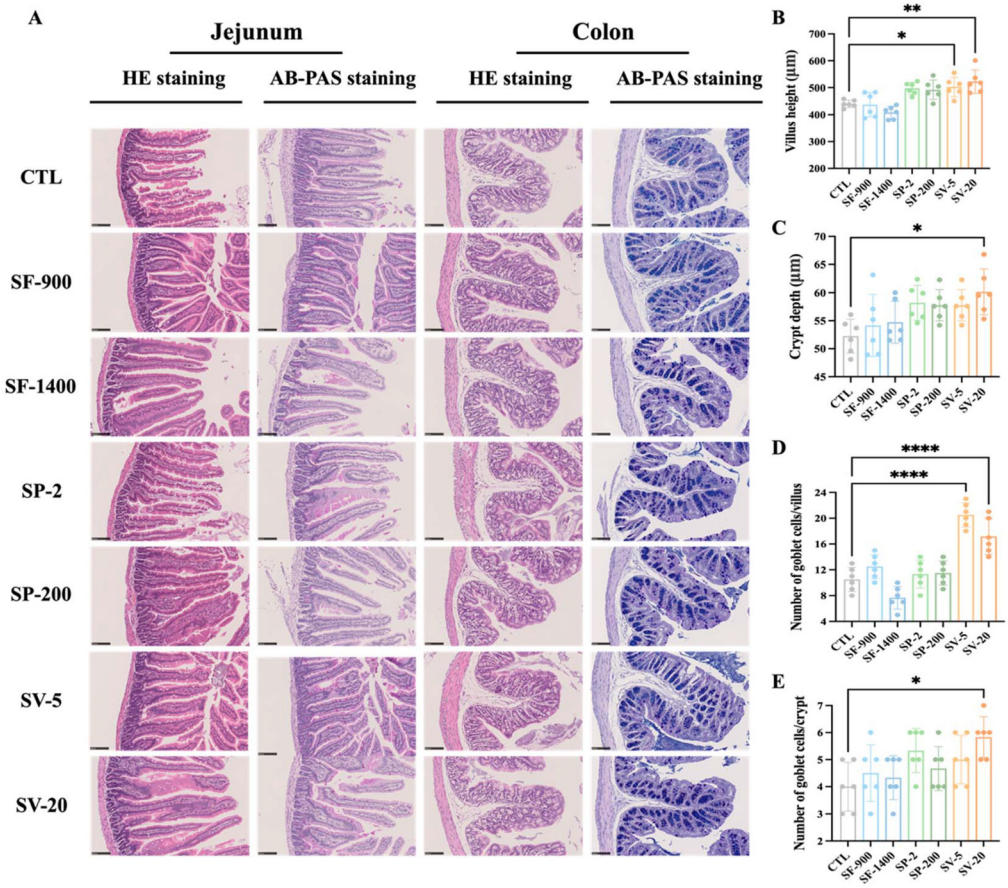

Fig. 4 The effects of SCFAs on intestinal morphology. (A) Representative HE staining and AB-PAS staining images of the jejunum and colon. (B) Villus length measured in the jejunum. (C) Crypt depth measured in the jejunum. (D) Number of goblet cells in each villus of the colon. (E) Number of goblet cells in each crypt of the colon. Data were expressed as mean ± standard deviation (mean ± SD), and differences between groups were assessed by one-way ANOVA followed by Tukey's multiple comparisons test: *$p < 0.05$, **$p < 0.01$, and ****$p < 0.0001$ ($n = 6$).

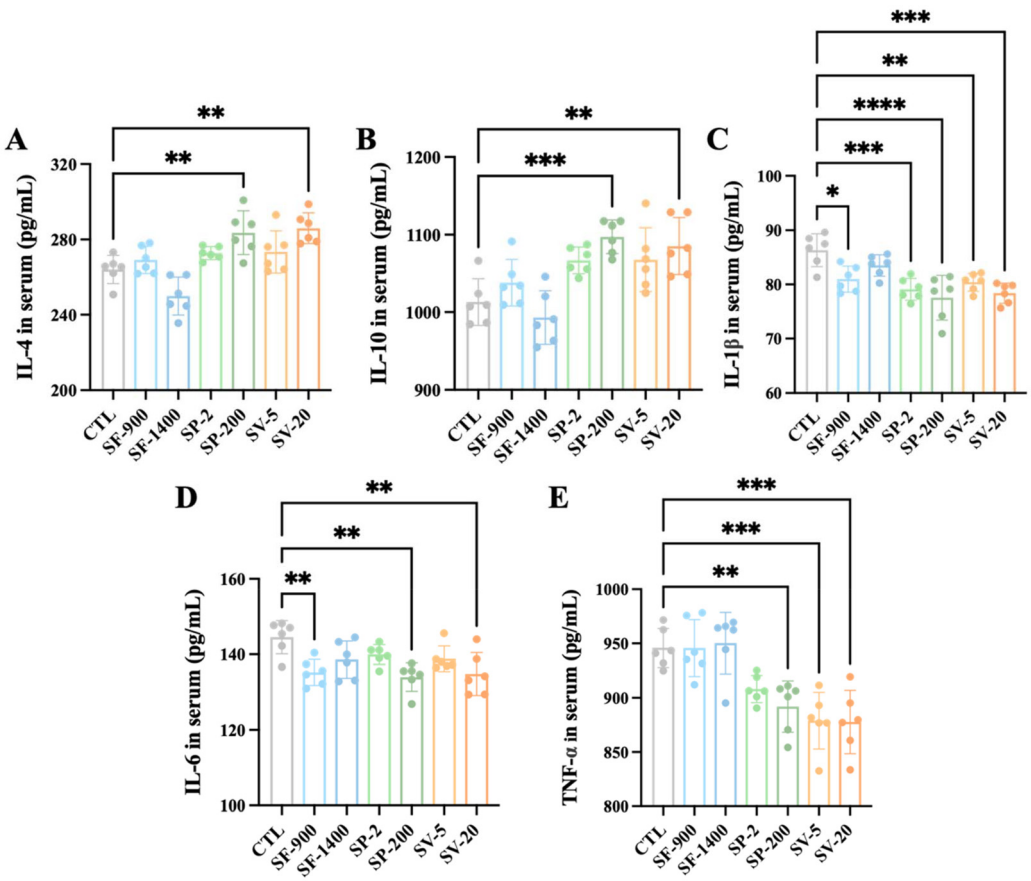

Fig. 5 Effects of SCFAs on serum inflammatory factors in neonatal mice. (A–E) Serum levels of IL-4, IL-10, IL-6, TNF-α, and IL-1 in each group of neonatal mice. Data were expressed as mean ± standard deviation (mean ± SD), and differences between groups were assessed by one-way ANOVA followed by Tukey's multiple comparisons test: *$p < 0.05$, **$p < 0.01$, ***$p < 0.001$, and ****$p < 0.0001$ ($n = 6$).

level, specific taxa were enriched in the SV-20 group, including *Lactobacillus*, *Alistipes*, and *Lachnospiraceae*_NK4A136_group (Fig. 6H). Furthermore, LEfSe analysis revealed bacterial taxa with significant differences between the treatment groups, with an LDA score >2.5 (Fig. 6I). In the SV-20 group, *Cyanobacteria*, *Lactobacillaceae*, and *Fructobacillus* were significantly enriched, whereas *Aerococcaceae*, *Aerococcus*, and *Parabacteroides* were enriched in the SV-5 group. Subsequent Wilcoxon analysis revealed a marked enrichment of several genera, including *Aerococcus*, *Fructobacillus*, *Proteus*, *Ralstonia*, *Vibrio*, *Pantoea*, and *Photobacterium* in the SV-20 group relative to controls (Fig. S2). KEGG-based functional prediction suggested treatment-associated shifts in the predicted microbial functional profile (Fig. S5). Several pathways showed distinct patterns across CTL, SV-5, and SV-20. These included predicted gene sets related to SCFA-associated carbon metabolism (*e.g.*, pyruvate and butanoate/propanoate metabolism), bile acid-related pathways, and cell envelope components (*e.g.*, lipopolysaccharide and peptidoglycan biosynthesis), as well as energy/redox-associated pathways (*e.g.*, lipoic acid metabolism and fatty acid degradation). These predicted patterns may be relevant to the improved barrier integrity and reduced circulating LPS observed in valerate-treated neonatal mice.

SCFAs promote bone development

To assess the impact of SCFA supplementation on skeletal development, femur length was measured. No significant intergroup differences were detected (Fig. 7A and B). Representative femoral micro-CT reconstructions are presented in Fig. 7C. Notably, valeric acid treatment significantly increased the bone volume to total volume ratio (BV/TV), BMD, trabecular number (Tb.N), and trabecular thickness (Tb.Th) (Fig. 7D–G). Conversely, the structure model index (SMI) was significantly reduced in both the SV-5 and SV-20 groups compared to the CTL group (Fig. 7H), indicating improved trabecular structure. However, no significant changes in trabecular separation (Tb.Sp) were observed across all groups (Fig. 7I).

SCFAs modulate bone metabolism

To further investigate the effect of SCFAs on bone metabolism, serum markers of bone turnover, including CTX, PINP, and the CTX/PINP ratio, were quantified using ELISA. PINP levels were significantly elevated in the SV-5 and SV-20 groups (Fig. 8A). In contrast, serum CTX levels and the CTX/PINP ratio remained stable across all groups (Fig. 8B and C), suggesting that valeric acid minimally influences bone resorption while preferentially promoting bone anabolism.

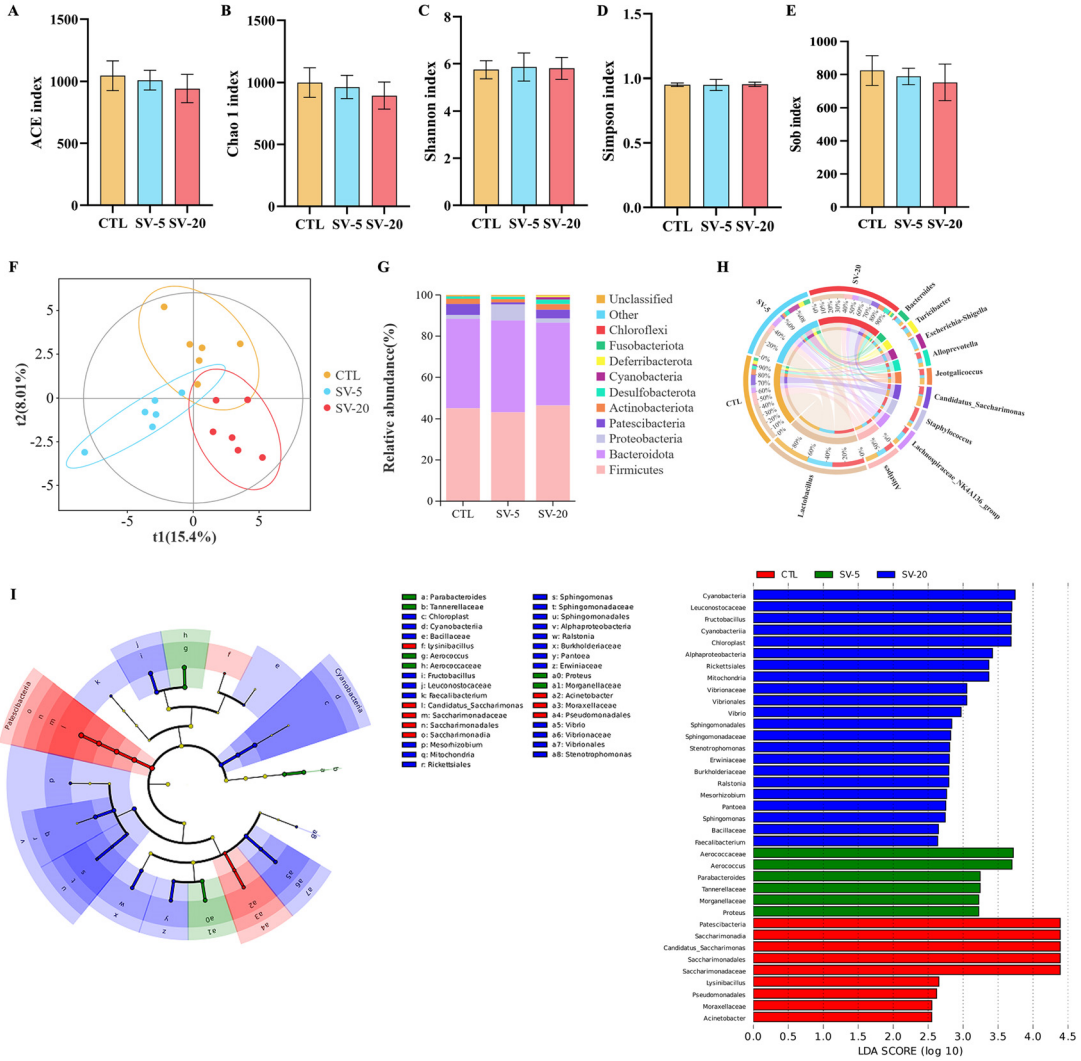

Fig. 6 Effect of valerate on intestinal microbiota in neonatal mice (n = 6). (A–D) Alpha-diversity of gut microbes (ACE, Chao1, Shannon, Simpson, and Sob). (E) Beta-diversity of gut microbes (PLS-DA analysis). (F) Circos diagram of microbial composition at the phylum level. (G) Stack diagram of genus horizontal species composition. (H and I) LEfSe analysis of intestinal bacteria in neonatal mice (LDA score and cladogram).

To explore the effect of SCFAs on osteogenesis-related genes, expression levels in the femur were examined. Runx2, a master regulator of osteoblast differentiation, was significantly upregulated in both the SV-5 and SV-20 groups compared to the CTL group (Fig. 8D). Similarly, FGFR1 expression, essential for osteoprogenitor proliferation and differentiation, was markedly increased in the valeric acid-treated groups (Fig. 8E). Additionally, growth hormone receptor (GHR) expression was significantly enhanced in the SV-20 group (Fig. 8F).

Relationships between the abundances of bacterial taxa, intestinal, and bone characteristics

Given that valeric acid produced the most pronounced improvements in intestinal barrier function and skeletal outcomes among the tested SCFAs, downstream microbiota–host association analyses were performed focusing on the CTL, SV-5, and SV-20 groups, for which matched microbiome sequencing data and the corresponding intestinal/bone phenotypes were available (Fig. 9). To investigate potential links between gut microbial taxa and host readouts, we examined correlations among bacterial composition, intestinal function markers, and bone parameters within these groups. The Mantel test identified significant positive correlations between the abundances of *Fructobacillus*, *Pantoea*, and *Ralstonia* and barrier-related genes in the colon and jejunum (Fig. 9A). Correlation analysis further revealed that the expression levels of barrier-related genes, goblet cell numbers, and intestinal length were positively correlated with bone development indices, while IL-1β and D-lactate levels were negatively correlated with these bone indices (Fig. 9B). Canonical correspondence analysis showed clear separation of microbial community structures among the CTL, SV-5, and SV-20 groups, indicating that microbial composition varied with treatment dosage. *Ralstonia*, *Fructobacillus*, *Pantoea*, and *Photobacterium*

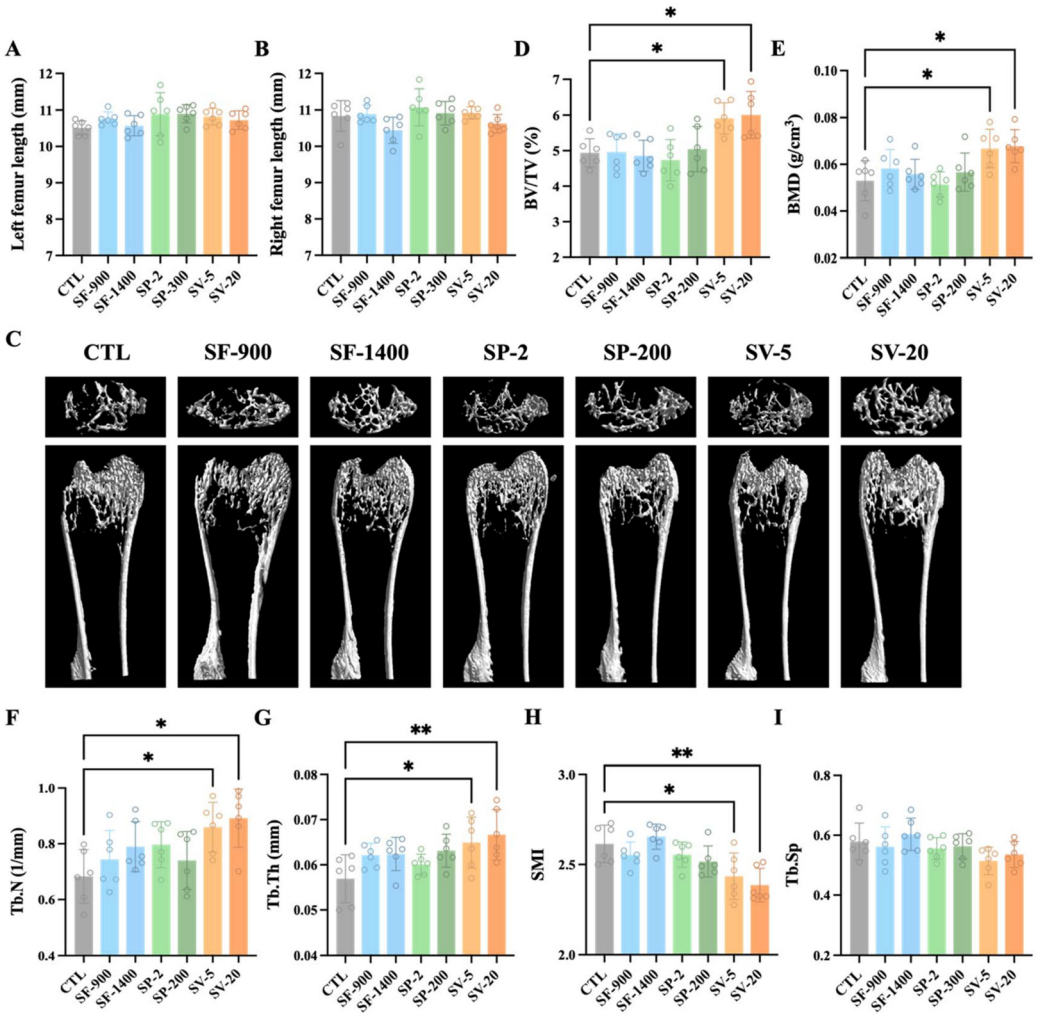

Fig. 7 Effects of SCFAs on skeletal development in neonatal mice. (A and B) The length of the left femur and the right femur. (C) Representative microscopy imaging (micro-CT). (D) Bone volume/total volume. (E) Bone mineral density. (F) Trabecular number. (G) Trabecular thickness. (H) Structure model index. (I) Trabecular separation. Data were expressed as mean ± standard deviation (mean ± SD), and differences between groups were assessed by one-way ANOVA followed by Tukey's multiple comparisons test: *$p < 0.05$, **$p < 0.01$, and ***$p < 0.001$ ($n = 6$).

exhibited strong associations with bone-related variables (Fig. 9C). Together, these analyses indicate that specific bacterial taxa and community patterns are associated with intestinal barrier-related readouts and bone parameters in the control and valerate-treated neonatal mice.

Discussion

Intestinal and skeletal developments during the neonatal period are tightly interlinked, laying the foundation for growth, nutrient utilization, and immune balance throughout life.[24,25] During early life, milk is the primary dietary input, and its composition varies across lactation and between sources, which may influence microbial colonization and metabolite production.[26,27] In this context, the gut microbiota and its metabolic products, particularly SCFAs, are increasingly recognized as key coordinators of gut–bone communication. In this study, we investigated the effects of three SCFAs, formate, propionate, and valerate, on intestinal and skeletal development in neonatal mice. Our results demonstrate that SCFA supplementation, especially valerate, promotes body growth, enhances intestinal structure and barrier integrity, regulates immune responses, reshapes gut microbial composition, and supports bone formation.

Among the three SCFAs tested, valerate (SV-5 and SV-20) and propionate (SP-2) were associated with greater increases in body weight in neonatal mice, consistent with previous findings in piglet models.[28] This growth-promoting effect is likely driven by enhanced intestinal function. Histological and morphometric analyses showed that SCFA treatment, particularly with valerate, significantly increased villus height, crypt depth, and goblet cell numbers, hallmarks of improved absorptive and secretory capacity. These structural changes not only expand the intestinal surface area for nutrient uptake but also strengthen mucosal protection through increased mucus secretion.[29,30]

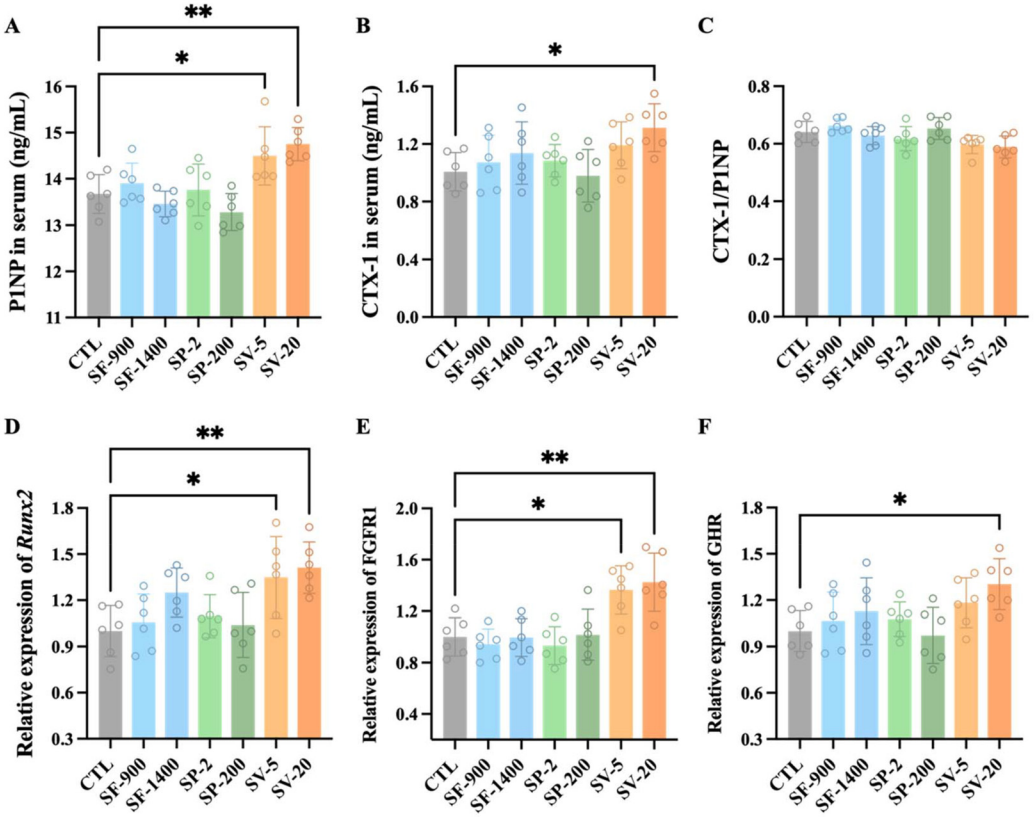

Fig. 8 Effects of SCFAs on the expression of bone transformation markers and osteogenic genes in neonatal mice. (A–C) Serum CTX, PINP and CTX-I/PINP contents. (D–F) Relative expression levels of Runx2, FGFR1, and GHR in the femur. Data were expressed as mean ± standard deviation (mean ± SD), and differences between groups were assessed by one-way ANOVA followed by Tukey's multiple comparisons test: *p < 0.05 and **p < 0.01 (n = 6).

Our observations align with earlier reports that SCFAs promote mucosal development and epithelial maturation in the gut.[29–31]

During early life, the immature intestinal barrier predisposes neonates to increased permeability and microbial translocation.[32] In our study, SCFA supplementation, particularly valerate, significantly improved barrier integrity, as evidenced by reduced FITC–dextran permeability and decreased serum levels of D-lactate and LPS. Valerate increased the expression levels of tight junction genes (claudin-1 and ZO-1) and mucin-related genes (MUC1 and MUC2) and increased goblet cell differentiation. These changes are believed to enhance epithelial defense and mucosal stability.[33] Nevertheless, the upstream signaling pathways underlying these effects remain to be elucidated and warrant further investigation.

In addition to enhancing the barrier function, SCFAs modulated mucosal immune responses. Valerate treatment significantly increased anti-inflammatory cytokines (IL-4 and IL-10) while suppressing pro-inflammatory mediators (IL-6 and TNF-α), suggesting a shift toward an anti-inflammatory immune state. This immune shift facilitates mucosal tolerance and safeguards intestinal development during early life.[34–36] These findings support previous evidence that SCFAs contribute to immune regulation and highlight their role in coordinating epithelial and immune maturation during early life.[31,37]

Importantly, valerate also exhibited anabolic effects on skeletal development. Micro-CT analysis showed significant increases in BV/TV, BMD, and Tb.Th in the SV-5 and SV-20 groups. These structural improvements were accompanied by elevated serum PINP levels and upregulated expression of osteogenic markers such as Runx2, FGFR1, and GHR, while bone resorption markers remained unchanged. These findings suggest that valerate promotes bone formation primarily by enhancing osteoblast activity. The anabolic effect may be partially mediated by improved intestinal calcium absorption and the activation of systemic IGF-1 signaling, mechanisms previously reported for other SCFAs.[19,38]

Emerging evidence suggests that these physiological effects may be partially mediated by shifts in gut microbial composition.[39–41] In our study, valerate supplementation reshaped microbiota profiles, particularly enriching genera such as *Fructobacillus*, *Pantoea*, and *Ralstonia* in the SV-20 group. These taxa are known to promote gut health through SCFA production, mucosal support, and immune modulation. *Fructobacillus* are obligately heterofermentative lactic acid bacteria that metabolize carbohydrates to produce SCFAs such as acetate and propionate, contributing to intestinal pH regulation and mucosal stability.[42] *Pantoea* has been associated with suppression of pathogenic microbes and maintenance

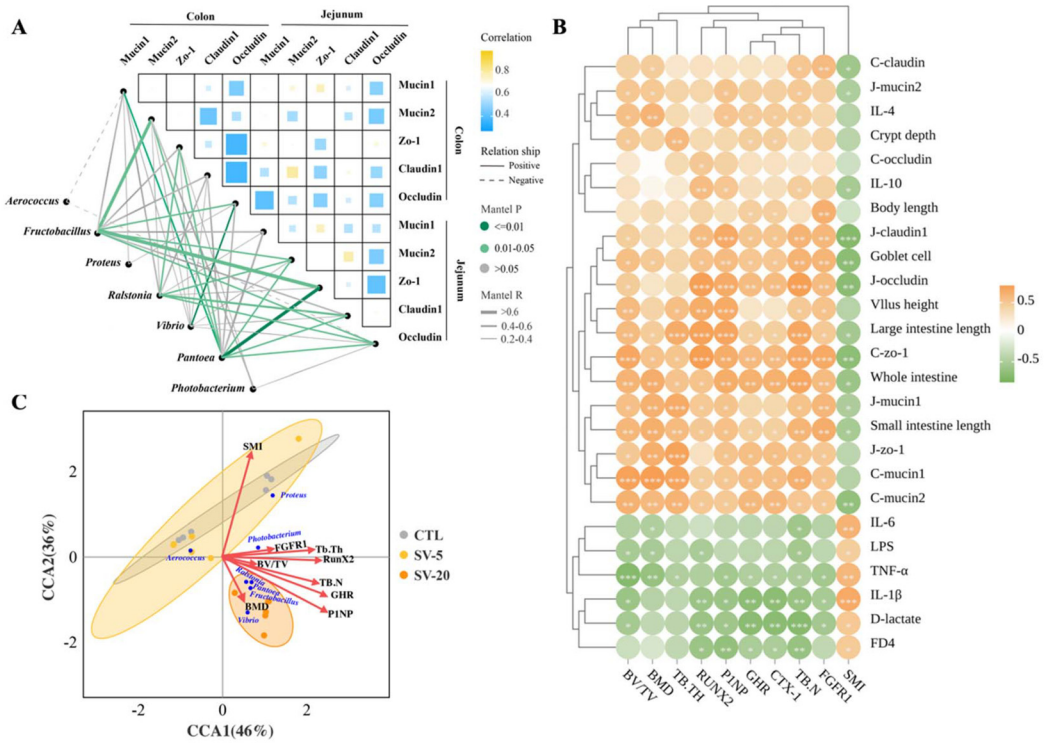

Fig. 9 Relationships between the abundances of intestinal microbial taxa and intestinal characteristics, and bone indices of the mice (n = 6). (A) Mantel's test correlations between the abundances of intestinal microbial taxa and the expression of genes related to intestinal barrier function. (B) Heatmap of the Pearson correlations of the abundances of intestinal indices and bone indices. (C) Distance-based redundancy analysis triplot showing the relationships of the abundances of intestinal microbial taxa and the bone indices.

of microbial homeostasis, likely through antimicrobial metabolite production and ecological competition,[43–45] However, *Ralstonia* are recognized as plant pathogens, and their role in mammalian gut ecosystems remains unclear and warrants further investigation.[46,47] Current evidence does not definitively support their roles in SCFA production or immune modulation; however, their enrichment may reflect either a microbial adaptation to valerate or host-mediated selection. These compositional changes suggest that SCFAs, particularly valerate, may shape microbial communities in ways that favor intestinal and immune development, although further mechanistic studies are needed to validate the functions of less-characterized taxa.

Correlation analysis further confirmed strong associations between specific bacterial taxa and both intestinal and skeletal parameters. The Mantel test revealed that *Fructobacillus*, *Pantoea*, and *Ralstonia* were positively correlated with intestinal barrier markers (*e.g.*, ZO-1 and MUC2), villus morphology, and bone indices such as BMD and trabecular number. These findings support the gut–bone axis model, suggesting that SCFA-induced microbial reshaping, particularly under valerate treatment, may mediate systemic developmental benefits. This aligns with previous reports that SCFAs promote beneficial microbes contributing to immune and metabolic homeostasis.[30,39]

Overall, our data show that SCFA supplementation, especially valerate, is associated with concurrent improvements in intestinal and skeletal outcomes in neonatal mice. These phenotypic changes occurred alongside increased barrier-related transcripts and morphology, shifts in mucosal immune-related readouts, and alterations in gut microbial community composition. However, the proposed gut–microbiota–barrier–bone framework in this study is primarily supported by association analyses, and the causal relationships among intermediate steps (*e.g.*, specific microbial metabolites, host signaling pathways, and barrier components at the protein level) remain to be determined. Our findings broaden the current understanding of SCFA biology in early life and support further investigation of microbiota-informed nutritional strategies to promote neonatal gut and bone health.

Limitations

Several limitations should be acknowledged. First, while SCFA supplementation produced clear phenotypic changes, the proposed gut microbiota–barrier–bone framework is supported mainly by associative analyses; key mechanistic intermediates were not directly assessed in the current study. Second, 16S rRNA profiling limits functional interpretation, and the observed taxa associations do not establish the causal contributions of individual genera. Third, these findings were obtained in neonatal mice under controlled conditions, and their generalizability to other developmental windows and to

humans remains to be determined. Future studies using targeted metabolite quantification and causal designs will be valuable to validate the proposed framework.

Author contributions

X. Y.: conceptualization, methodology, investigation, formal analysis, writing – original draft, and writing – review and editing. X. K. L.: conceptualization, methodology, formal analysis, and writing – review and editing. X. Z.: methodology and formal analysis. L. M.: writing – review and editing. J. Q. W.: funding acquisition and project administration. N. Z.: project administration and supervision.

Conflicts of interest

The authors declare no conflicts of interest.

Data availability

Raw data for gene sequencing described in this manuscript have been submitted to the NCBI BioProject under accession number PRJNA1301056. The data can be accessed at https://www.ncbi.nlm.nih.gov/bioproject/PRJNA1301056.

Supplementary information (SI) is available. See DOI: https://doi.org/10.1039/d5fo05394c.

Acknowledgements

This research was supported by the National Key R&D Program of China (2022YFD1301000), the earmarked fund for the China Agriculture Research System (CARS-36), and the Agricultural Science and Technology Innovation Program (ASTIP-IAS12).

References

1 A. L. Kau, P. P. Ahern, N. W. Griffin, A. L. Goodman and J. I. Gordon, Human nutrition, the gut microbiome and the immune system, *Nature*, 2011, **474**, 327–336.
2 X. Xu, X. Jia, L. Mo, C. Liu, L. Zheng, Q. Yuan and X. Zhou, Intestinal microbiota: a potential target for the treatment of postmenopausal osteoporosis, *Bone Res.*, 2017, **5**, 17046.
3 C. Ohlsson and K. Sjogren, Effects of the gut microbiota on bone mass, *Trends Endocrinol. Metab.*, 2015, **26**, 69–74.
4 A. Koh, F. De Vadder, P. Kovatcheva-Datchary and F. Backhed, From Dietary Fiber to Host Physiology: Short-Chain Fatty Acids as Key Bacterial Metabolites, *Cell*, 2016, **165**, 1332–1345.
5 J. Tan, C. McKenzie, M. Potamitis, A. N. Thorburn, C. R. Mackay and L. Macia, The role of short-chain fatty acids in health and disease, *Adv. Immunol.*, 2014, **121**, 91–119.
6 D. Parada Venegas, M. K. De la Fuente, G. Landskron, M. J. Gonzalez, R. Quera, G. Dijkstra, H. J. M. Harmsen, K. N. Faber and M. A. Hermoso, Short Chain Fatty Acids (SCFAs)-Mediated Gut Epithelial and Immune Regulation and Its Relevance for Inflammatory Bowel Diseases, *Front. Immunol.*, 2019, **10**, 277.
7 S. Lucas, Y. Omata, J. Hofmann, M. Bottcher, A. Iljazovic, K. Sarter, O. Albrecht, O. Schulz, B. Krishnacoumar, G. Kronke, M. Herrmann, D. Mougiakakos, T. Strowig, G. Schett and M. M. Zaiss, Short-chain fatty acids regulate systemic bone mass and protect from pathological bone loss, *Nat. Commun.*, 2018, **9**, 55.
8 A. M. Tyagi, M. Yu, T. M. Darby, C. Vaccaro, J. Y. Li, J. A. Owens, E. Hsu, J. Adams, M. N. Weitzmann, R. M. Jones and R. Pacifici, The Microbial Metabolite Butyrate Stimulates Bone Formation via T Regulatory Cell-Mediated Regulation of WNT10B Expression, *Immunity*, 2018, **49**, 1116–1131.
9 A. Salhotra, H. N. Shah, B. Levi and M. T. Longaker, Mechanisms of bone development and repair, *Nat. Rev. Mol. Cell Biol.*, 2020, **21**, 696–711.
10 H. Wopereis, R. Oozeer, K. Knipping, C. Belzer and J. Knol, The first thousand days - intestinal microbiology of early life: establishing a symbiosis, *Pediatr. Allergy Immunol.*, 2014, **25**, 428–438.
11 L. W. Peterson and D. Artis, Intestinal epithelial cells: regulators of barrier function and immune homeostasis, *Nat. Rev. Immunol.*, 2014, **14**, 141–153.
12 X. Feng and J. M. McDonald, Disorders of bone remodeling, *Annu. Rev. Pathol.*, 2011, **6**, 121–145.
13 S. M. Holmberg, R. H. Feeney, P. K. V. Prasoodanan, F. Puertolas-Balint, D. K. Singh, S. Wongkuna, L. Zandbergen, H. Hauner, B. Brandl, A. I. Nieminen, T. Skurk and B. O. Schroeder, The gut commensal Blautia maintains colonic mucus function under low-fiber consumption through secretion of short-chain fatty acids, *Nat. Commun.*, 2024, **15**, 3502.
14 E. R. Mann, Y. K. Lam and H. H. Uhlig, Short-chain fatty acids: linking diet, the microbiome and immunity, *Nat. Rev. Immunol.*, 2024, **24**, 577–595.
15 C. Martin-Gallausiaux, L. Marinelli, H. M. Blottiere, P. Larraufie and N. Lapaque, SCFA: mechanisms and functional importance in the gut, *Proc. Nutr. Soc.*, 2021, **80**, 37–49.
16 M. Li, Q. Li, R. Abdlla, *et al.*, Donkey whey proteins ameliorate dextran sulfate sodium-induced ulcerative colitis in mice by downregulating the S100A8-TRAF6-NF-κB axis-mediated inflammatory response, *Food Sci. Hum. Wellness*, 2023, **12**, 1809–1819.
17 S. L. Bridgman, M. B. Azad, C. J. Field, A. M. Haqq, A. B. Becker, P. J. Mandhane, P. Subbarao, S. E. Turvey, M. R. Sears, J. A. Scott, D. S. Wishart, A. L. Kozyrskyj and C. S. Investigators, Fecal Short-Chain Fatty Acid Variations by Breastfeeding Status in Infants at 4 Months: Differences in Relative versus Absolute Concentrations, *Front. Nutr.*, 2017, **4**, 11.

18 H. Zeng, C. Huang, S. Lin, M. Zheng, C. Chen, B. Zheng and Y. Zhang, Lotus Seed Resistant Starch Regulates Gut Microbiota and Increases Short-Chain Fatty Acids Production and Mineral Absorption in Mice, *J. Agric. Food Chem.*, 2017, **65**, 9217–9225.

19 J. Yan, J. W. Herzog, K. Tsang, C. A. Brennan, M. A. Bower, W. S. Garrett, B. R. Sartor, A. O. Aliprantis and J. F. Charles, Gut microbiota induce IGF-1 and promote bone formation and growth, *Proc. Natl. Acad. Sci. U. S. A.*, 2016, **113**, E7554–E7563.

20 L. Xiao, Y. Zhou, S. Bokoliya, Q. Lin and M. Hurley, Bone loss is ameliorated by fecal microbiota transplantation through SCFA/GPR41/IGF1 pathway in sickle cell disease mice, *Sci. Rep.*, 2022, **12**, 20638.

21 Nature Research Custom. The early life of the gut microbiota. Nature (Partner Content). 2024, Accessed 12 Jan 2026. DOI: 10.1038/d42473-024-00330-w.

22 D. Han, W. Wang, J. Gong, Y. Ma and Y. Li, Microbiota metabolites in bone: Shaping health and Confronting disease, *Heliyon*, 2024, **10**, e28435.

23 L. Huertas-Diaz, M. E. Gezer, A. Marietou, J. Hosek, L. Thams, L. B. Dalgaard, M. Hansen and C. Schwab, Megasphaera contributes to lactate-driven valerate production in the human gut, *Microbiome*, 2025, **13**, 210.

24 O. D. Cooney, P. R. Nagareddy, A. J. Murphy and M. K. S. Lee, Healthy Gut, Healthy Bones: Targeting the Gut Microbiome to Promote Bone Health, *Front. Endocrinol.*, 2020, **11**, 620466.

25 S. Perrone, C. Caporilli, F. Grassi, M. Ferrocino, E. Biagi, V. Dell'Orto, V. Beretta, C. Petrolini, L. Gambini, M. E. Street, A. Dall'Asta, T. Ghi and S. Esposito, Prenatal and Neonatal Bone Health: Updated Review on Early Identification of Newborns at High Risk for Osteopenia, *Nutrients*, 2023, **15**(16), 3515.

26 M. Li, Q. Li, S. Kang, X. Cao, Y. Zheng, J. Wu, R. Wu, J. Shao, M. Yang and X. Yue, Characterization and comparison of lipids in bovine colostrum and mature milk based on UHPLC-QTOF-MS lipidomics, *Food Res. Int.*, 2020, **136**, 109490.

27 J. Chen, Y. Zhang, Z. Liu, J. Wang, S. Zhang, J. Shao, X. Yue and M. Li, Comprehensive characterization and comparison of polar lipids in bovine and donkey Milk based on Lipidomics, *Food Chem.*, 2025, **496**, 146801.

28 L. Kovanda, J. Park, S. Park, K. Kim, X. Li and Y. Liu, Dietary butyrate and valerate glycerides impact diarrhea severity and immune response of weaned piglets under ETEC F4-ETEC F18 coinfection conditions, *J. Anim. Sci.*, 2023, **101**, skad401.

29 J. Ma, X. Piao, S. Mahfuz, S. Long and J. Wang, The interaction among gut microbes, the intestinal barrier and short chain fatty acids, *Anim. Nutr.*, 2022, **9**, 159–174.

30 D. Rios-Covian, P. Ruas-Madiedo, A. Margolles, M. Gueimonde, C. G. de Los Reyes-Gavilan and N. Salazar, Intestinal Short Chain Fatty Acids and their Link with Diet and Human Health, *Front. Microbiol.*, 2016, **7**, 185.

31 Y. Zhang, H. Chen, W. Zhu and K. Yu, Cecal Infusion of Sodium Propionate Promotes Intestinal Development and Jejunal Barrier Function in Growing Pigs, *Animals*, 2019, **9**(6), 284.

32 B. Westrom, E. Arevalo Sureda, K. Pierzynowska, S. G. Pierzynowski and F. J. Perez-Cano, The Immature Gut Barrier and Its Importance in Establishing Immunity in Newborn Mammals, *Front. Immunol.*, 2020, **11**, 1153.

33 H. B. Wang, P. Y. Wang, X. Wang, Y. L. Wan and Y. C. Liu, Butyrate enhances intestinal epithelial barrier function via up-regulation of tight junction protein Claudin-1 transcription, *Dig. Dis Sci.*, 2012, **57**, 3126–3135.

34 N. Arpaia, C. Campbell, X. Fan, S. Dikiy, J. van der Veeken, P. deRoos, H. Liu, J. R. Cross, K. Pfeffer, P. J. Coffer and A. Y. Rudensky, Metabolites produced by commensal bacteria promote peripheral regulatory T-cell generation, *Nature*, 2013, **504**, 451–455.

35 Y. Furusawa, Y. Obata, S. Fukuda, T. A. Endo, G. Nakato, D. Takahashi, Y. Nakanishi, C. Uetake, K. Kato, T. Kato, M. Takahashi, N. N. Fukuda, S. Murakami, E. Miyauchi, S. Hino, K. Atarashi, S. Onawa, Y. Fujimura, T. Lockett, J. M. Clarke, D. L. Topping, M. Tomita, S. Hori, O. Ohara, T. Morita, H. Koseki, J. Kikuchi, K. Honda, K. Hase and H. Ohno, Commensal microbe-derived butyrate induces the differentiation of colonic regulatory T cells, *Nature*, 2013, **504**, 446–450.

36 M. A. Vinolo, H. G. Rodrigues, R. T. Nachbar and R. Curi, Regulation of inflammation by short chain fatty acids, *Nutrients*, 2011, **3**, 858–876.

37 H. Diao, A. R. Jiao, B. Yu, X. B. Mao and D. W. Chen, Gastric infusion of short-chain fatty acids can improve intestinal barrier function in weaned piglets, *Genes Nutr.*, 2019, **14**, 4.

38 J. Yan, A. Takakura, K. Zandi-Nejad and J. F. Charles, Mechanisms of gut microbiota-mediated bone remodeling, *Gut Microbes*, 2018, **9**, 84–92.

39 X. Lin, H. M. Xiao, H. M. Liu, W. Q. Lv, J. Greenbaum, R. Gong, Q. Zhang, Y. C. Chen, C. Peng, X. J. Xu, D. Y. Pan, Z. Chen, Z. F. Li, R. Zhou, X. F. Wang, J. M. Lu, Z. X. Ao, Y. Q. Song, Y. H. Zhang, K. J. Su, X. H. Meng, C. L. Ge, F. Y. Lv, Z. Luo, X. M. Shi, Q. Zhao, B. Y. Guo, N. J. Yi, H. Shen, C. J. Papasian, J. Shen and H. W. Deng, Gut microbiota impacts bone via Bacteroides vulgatus-valeric acid-related pathways, *Nat. Commun.*, 2023, **14**, 6853.

40 P. D'Amelio and F. Sassi, Gut Microbiota, Immune System, and Bone, *Calcif. Tissue Int.*, 2018, **102**, 415–425.

41 F. A. Vicentini, C. M. Keenan, L. E. Wallace, C. Woods, J. B. Cavin, A. R. Flockton, W. B. Macklin, J. Belkind-Gerson, S. A. Hirota and K. A. Sharkey, Intestinal microbiota shapes gut physiology and regulates enteric neurons and glia, *Microbiome*, 2021, **9**, 210.

42 A. Endo, S. Maeno, Y. Tanizawa, W. Kneifel, M. Arita, L. Dicks and S. Salminen, Fructophilic Lactic Acid Bacteria, a Unique Group of Fructose-Fermenting Microbes, *Appl. Environ. Microbiol.*, 2018, **84**(19), e01290–18.

43 W. T. Yang, Y. J. Yi and B. Xia, Unveiling the duality of Pantoea dispersa: A mini review, *Sci. Total Environ.*, 2023, **873**, 162320.

44 A. Kirk, E. Davidson and J. Stavrinides, The expanding antimicrobial diversity of the genus Pantoea, *Microbiol. Res.*, 2024, **289**, 127923.
45 S. Shetty, A. Kamble and H. Singh, Insights into the Potential Role of Plasmids in the Versatility of the Genus Pantoea, *Mol. Biotechnol.*, 2024, **66**, 3398–3414.
46 N. Peeters, A. Guidot, F. Vailleau and M. Valls, Ralstonia solanacearum, a widespread bacterial plant pathogen in the post-genomic era, *Mol. Plant Pathol.*, 2013, **14**, 651–662.
47 K. Rivera-Zuluaga, R. Hiles, P. Barua, D. Caldwell and A. S. Iyer-Pascuzzi, Getting to the root of Ralstonia invasion, *Semin. Cell Dev. Biol.*, 2023, **148–149**, 3–12.